

This paper was recommended for publication in revised form by Editor in Chief Ahmet Selim Dalkilic

HEAT TRANSFER PERFORMANCE OF SILVER/WATER NANOFLUID IN A SOLAR FLAT-PLATE COLLECTOR

Siddharth Roy

Department of Mechanical Engineering, Karunya
University
Coimbatore 641114, Tamil Nadu, India

Lazarus Godson Asirvatham*

Department of Mechanical Engineering, Karunya
University
Coimbatore 641114, Tamil Nadu, India

Deepak Kunhappan

Department of Mechanical
Engineering, Karunya University
Coimbatore 641114, Tamil Nadu,
India

Enoch Cephas

Department of Mechanical
Engineering, Karunya University
Coimbatore 641114, Tamil Nadu,
India

Somchai Wongwises

Fluid Mechanics, Thermal
Engineering and Multiphase
Flow Research Lab (FUTURE),
Department of Mechanical
Engineering, Faculty of
Engineering, King Mongkut's
University of Technology
Thonburi, Bangmod, Bangkok
10140, Thailand

Keywords: silver; nanoparticles, solar flat plate collector, convection, heat transfer.

** Corresponding author: Lazarus Godson Asirvatham, Phone: +91 422 2614430, Fax: +91 422 2615615
E-mail address: godson@karunya.edu, godasir@yahoo.co.in*

ABSTRACT

An experimental study is carried out to investigate the heat transfer characteristics of silver/water nanofluid in a solar flat-plate collector. The solar radiation heat flux varies between 800 W/m² and 1000 W/m², and the particle concentration varies between 0.01%, 0.03%, and 0.04%. The fluid Reynolds number varies from 5000 to 25000. The influence of radiation heat flux, mass flow rate of nanofluid, inlet temperature into the solar collector, and volume concentration of the particle on the convective heat transfer coefficient and the collector efficiency are studied. Both parameters increase with increase in the particle volume concentration and flow rate. The maximum percentage increase obtained in the convective heat transfer coefficient is 18.4% for the 0.04% volume concentration at a Reynolds number of 25000. An increase in the performance of nanofluid is also witnessed when compared to the base fluid, which has a strong dependency on volume concentration and mass flow rate.

1. INTRODUCTION

Suspension of nano-particles in a conventional heat transfer fluids [1-4] results in notable enhanced thermal properties. These properties of thermal conductivity, thermal diffusivity, viscosity, and design parameter for convective heat transfer are enhanced in comparison to base fluid properties [5-8], and these results would be beneficial in saving equipment costs and increasing performance. Wong and De Leon [9] carried out a review paper detailing the current and future applications of nanofluids. The need for economical, energy-efficient, and technologically sustainable green technologies is being met by nanofluids in many key applications to control the flow of heat [10], cool nuclear reactors [11], and cool microchips [12], etc. Experimental investigations on the application of nanofluids in solar energy has been done as well [13].

Li et al. [14] investigated the forced convective heat transfer of nanofluids in solar collectors during the day and night, with distilled water and nanoparticles of Al₂O₃, ZnO, and

MgO. The nanofluid achieved a 3°C temperature difference during the daytime peak solar radiation compared with the base fluids. With a concentration of 0.2% ZnO, a temperature difference of 2.55°C for daytime and 1°C for nighttime was reached, and this was determined to be the most attractive option for solar energy utilization. Yousefi et al. [15] witnessed a 28% performance improvement in a flat-plate collector when it was operated with water-Al₂O₃ nanofluids. Tyagi [16] theoretically compared the conventional flat-plate collector with a direct absorption solar collector (DAC) and observed the former to be 10% more efficient. Otanicar [17] studied the economic and environmental influences of using nanofluids to enhance solar collector efficiency with conventional solar collectors. Dongxiao et al. [18] presented excellent photo-thermal properties of carbon-black aqueous nanofluids at high-volume fractions. Further work on nanofluids' application to direct solar absorption has been carried out by Lijuan Mu [19] using a custom-made direct solar absorber. The radiative properties of several nanofluids are tested for the highest temperature difference across the heat exchangers.

Based on the above-mentioned review of the literature, it has been clearly observed that most of the previous studies on solar flat-plate collectors were conducted using metal oxide nanoparticles in relatively high concentrations. These high concentrations of metal oxide nanoparticles cause a higher pressure drop that then requires a higher pumping power. Since a limited number of studies exists in the literature with respect to pure metal nanoparticles, it is recommended to study the heat transfer characteristics of pure metal nanoparticles with relatively low concentrations (<1%) by volume and high thermal conductivity compared with metal oxides. Therefore, in the present study, the efficiency of a solar flat-plate collector is studied with a low particle volume concentration of less than 0.04% silver-water nanofluid. These experiments are conducted for a solar radiation flux ranging from 800 W/m² to 1000 W/m², and the Reynolds number varying from 5000 to 25000. The effect of radiative heat flux, mass flow rate, inlet temperature, and volume concentration on the convective heat transfer coefficient and the collector efficiency are studied. The tailor-made setup for a collector area is 2.4m² and the collector plate is made of nine parallel copper strips.

2. EXPERIMENTS

2.1 Nanofluid preparation

Silver nanofluids with particle volume concentrations of 0.01%, 0.03%, and 0.04% are prepared by suspending the required amount of silver nanoparticles in water with polyvinyl pyrrolidone (PVP) used as the surfactant. The mixture is composed of Ag (silver) nanoparticles with an average diameter of less than 100 nm and PVP dispersed in water. In order to produce the required particle volume fractions, a dilution with water followed by a stirring action was used. Moreover, an ultrasonic vibrator with a frequency range from 0 Hz to 100 Hz is used to sonicate the solution continuously for approximately

30 minutes in order to break down the agglomeration of nanoparticles. The Scanning Electron Microscope (SEM) analysis has been done to observe the size and morphology of the suspended silver nanoparticles.

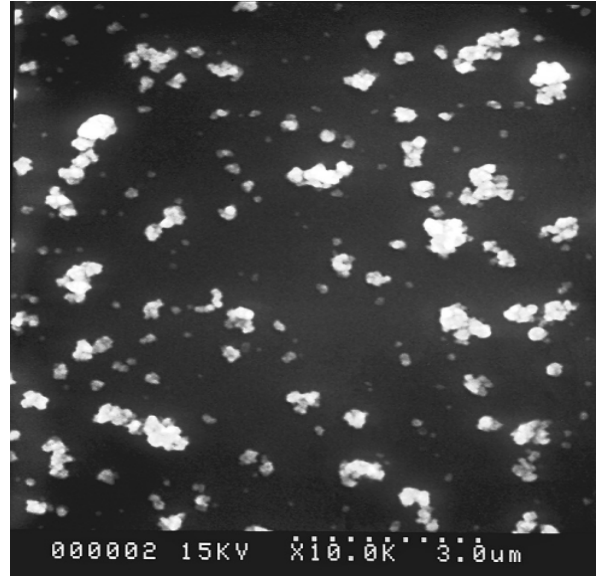


FIGURE 1. SEM IMAGE OF 0.04% VOLUME CONCENTRATION OF SILVER/WATER NANOFUID

Fig 1 shows the 0.04 % volume concentration of silver/water nanofluid taken at 10X magnification. It is clearly observed from Fig 1 that the silver nanoparticles are uniformly dispersed and have size of less than 100 nm. The thermo physical properties of the nanofluid are calculated as follows: density by Pak and Cho [21], thermal conductivity by Yu and Choi [22], viscosity by Einstein's equation [23]. The specific heat of the nanofluid is calculated by Xuan and Roetzel [24].

$$\rho_{nf} = \Phi \rho_p + (1 - \Phi) \rho_w \quad (1)$$

$$\mu_{nf} = (1 + 2.5\Phi) \mu_w \quad (2)$$

$$k_{nf} = \left[\frac{k_p + 2k_w + 2(k_p - k_w)(1 + \beta)^3 \Phi}{k_p + 2k_w - (k_p - k_w)(1 + \beta)^3 \Phi} \right] k_w \quad (3)$$

$$(\rho C_p)_{nf} = \phi(\rho C_p)_p + (1 - \phi)(\rho C_p)_w \quad (4)$$

In these equations, ρ_{nf} is the density of the nanofluid, ρ_p the density of nanoparticle, and ρ_w the density of water. μ represents viscosity, k thermal conductivity, C_p specific heat, and the subscripts w and p are the properties of water and nanoparticles. Here Φ is the volume concentration of the nanofluid. The uncertainty analysis is done using the method proposed by Robert J. Moffat [25] and the maximum error in

the observed readings and calculated parameters are found to be less than $\pm 5\%$.

2.2 Experimental setup

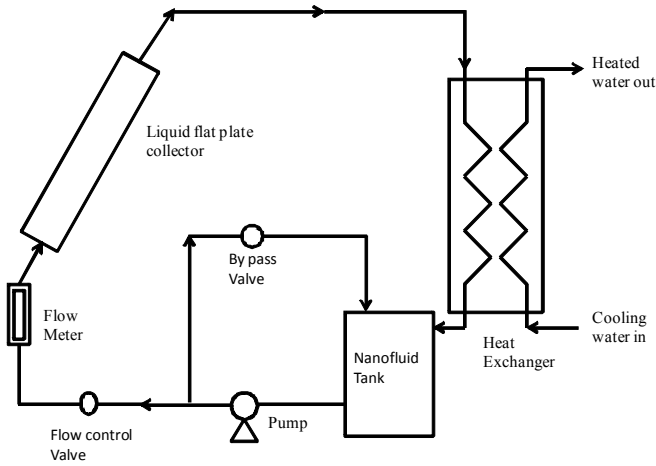


FIGURE 2a . SCHEMATIC DIAGRAM OF THE EXPERIMENTAL LAYOUT



FIGURE 2 b. PHOTOGRAPHIC VIEW OF THE TEST SECTION

The schematic diagram of the test facility (figure 2a) is a closed loop consisting of a flat-plate collector, liquid pump, heat exchanger, and storage tank. A bypass valve is provided around the pump so that the mass flow rate can be adjusted to the prescribed value. The heat exchanger is used to eliminate heat from the outlet water. The combination of a heat exchanger and a storage tank enables the user to adjust the fluid inlet temperature. A set of 27 K-type thermocouples (figure 2b) with $\pm 0.1\%$ accuracy are attached at several pre-determined positions of the riser tubes to measure the wall temperature of the collector. Two K-type thermocouples are immersed in the

fluid to measure the bulk fluid temperatures between the inlet and outlet of the test section. A pyranometer with a digital micro-voltmeter is used to determine the incident radiation on the flat-plate collector, and two pressure sensors with $\pm 0.1\%$ accuracy are immersed in the fluid between the inlet and outlet of the collector to measure the pressure drop. For the detailed specifications of the collector, see table 1.

TABLE 1. SPECIFICATIONS OF THE SOLAR FLAT PLATE COLLECTOR

Specifications	Dimensions
Occupied area	200mm x 120mm x 15mm
Absorber area	190mm x 115mm
Header pipe (Cu)	Φ 25.4mm
Connector riser pipe	Φ 12.5mm
Absorber sheet (Cu)	---

The experiments are conducted according to the ASHRAE 93-86 [20] testing of solar flat-plate collectors. The standard specifies that the collector will be tested under clear-sky conditions to determine its efficiency characteristics. On any given day, data is recorded under steady-state conditions for fixed values of mass flow rate and fluid inlet temperature. The collector is considered to be operating under steady-state conditions if the deviation of the experimental readings observed for a given mass flow rate is less than the following specified limits over a 15-minute time period:

Global radiation incident on collector plane	$\pm 50 \text{ W/m}^2$
Ambient temperature	$\pm 1^\circ\text{C}$
Fluid flow rate	$\pm 1\%$
Fluid inlet temperature	$\pm 0.1^\circ\text{C}$
Temperature rise across the collector	$\pm 0.1^\circ\text{C}$

Other specification are that the value of total radiation I_T is greater than 600 W/m^2 , the wind speed between 3 m/s and 6 m/s, and the fluid flow rate at approximately 0.02 kg/s per square meter of collector gross area. With respect to the present study, the maximum variation in total/global radiation observed is 15 W/m^2 , which is still far less than the value given in the ASHRAE standards. While the maximum variations between the inlet and outlet temperatures are found to be less than 1°C . The wind velocity measured with the anemometer vary between 3m/s and 5 m/s. The solar collector is tested for various mass flow rates varying from 1 L/min to 10 L/min with corresponding Reynolds numbers ranging from 5000 to 25000; however, the efficiency calculations are limited to a flow rate of 6 L/min and each reading is taken at 15-minute time intervals. During the experimental test runs, the mass flow rate, incident radiation, wall temperatures, inlet and outlet fluid temperatures,

and wind velocity are observed and stored in the data log for further processing and data reduction.

2.3 Data reduction and efficiency calculation

The incident radiation or total radiation, I_T , is determined by a pyranometer. The useful q_u heat gain is then calculated as

$$Q_u = A_p S - Q_l \quad (5)$$

$$Q_l = U_l A_p (T_{pm} - T_a) \quad (6)$$

$$S = I_T (\tau\alpha) \quad (7)$$

where A_p is the collector plate area, S is the absorbed radiation, q_l is the heat loss by convection and re-radiation, U_l is the overall loss coefficient, T_{pm} is the mean plate temperature of the absorber plate, T_a is the ambient temperature, and $\tau\alpha$ stands for the absorbance transmittance product.

The convective heat transfer coefficient of the fluid is determined by the following equations. From the useful heat gain equation, the heat flux on the riser tube is calculated as:

$$q_u = \frac{Q_u}{A_t} \quad (8)$$

where A_t is the lateral surface area of the riser tube.

The fluid temperature corresponding to the measured wall temperature is calculated as:

$$T_{fi} = T_w - \left(\frac{Q_u \ln\left(\frac{r_1}{r_2}\right)}{2\pi k l_i} \right) \quad (9)$$

The bulk fluid temperature is calculated as:

$$T_b = \frac{T_i + T_{fi}}{2} \quad (10)$$

The Reynolds number is calculated by the equation:

$$Re_{nf} = \frac{\rho_{nf} u D}{\mu_{nf}} \quad (11)$$

The convective heat transfer coefficient is then calculated by the equation:

$$h_{nf} = \frac{q_u}{T_{w(nf)} - T_{b(nf)}} \quad (12)$$

The Nusselt number for the nanofluid is given as:

$$Nu_{nf} = \frac{h_{nf} D}{k_{nf}} \quad (13)$$

The efficiency of the flat-plate collector can be defined by:

$$\eta_i = \frac{Q_u}{A_c I_T} = \frac{m C_p (T_{fo} - T_{fi})}{A_c I_T} \quad (14)$$

Equation number 14 can be further modified in terms of the heat removal factor F_R :

$$\eta_i = F_R (\tau\alpha) - F_R U_L \frac{T_{fi} - T_a}{I_T} \quad (15)$$

The calculated efficiencies are then plotted with the parameter $((T_{fi} - T_a) / I_T) \times 1000$. The experimental values of efficiency are plotted against the parameter $((T_{fi} - T_a) / I_T) \times 1000$ and generally yield straight lines; however, the scatter of the experimental data is found to be less than $\pm 10\%$ deviation.

3. RESULTS AND DISCUSSION

The experimental test facility is validated for its accuracy by conducting some preliminary experiments with water. The experimental Nusselt number obtained from the present study are compared with the Dittus–Boelter correlation [26]. A deviation of $\pm 9\%$ is observed between the experimental results and those obtained by the correlation, thus validating the experimental setup's accuracy. The variations of temperature over time with incident solar radiation of 900W/m^2 are shown in figure 3.

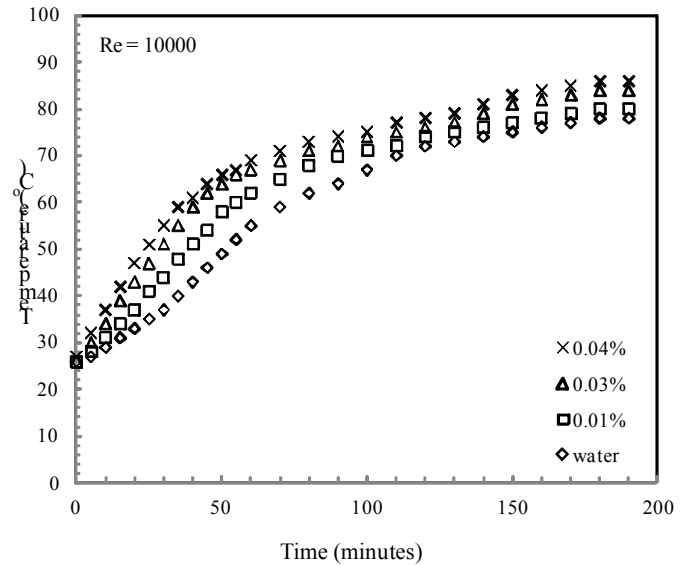


FIGURE 3. EVOLUTION OF FLUID TEMPERATURE PROFILE WITH RESPECT TO TIME IN SOLAR COLLECTOR

The temperature rise of the nanofluid across the collector over time is higher when compared to that of the base fluid. For the particle concentration of 0.04%, the nanofluid has the highest temperature rise of 4°C. Nanofluids are known to have higher heat absorption capabilities compared to that of water as the dispersed nanoparticles tend to absorb more incident energy due to the pure metallic nature and higher thermal conductivity [16]. The wall and bulk fluid temperatures for various particle concentrations are shown in figure 4.

The particle concentration is observed to have an indirect relation with the wall temperature; for instance, a decrease of 3°C is observed for the $\phi = 0.04\%$ concentration. This effect on the decreased wall temperature can be attributed to the fact that on suspending silver nanoparticles in the base fluid, the thermo-physical properties of the resulting mixture are improved. The bulk fluid temperature recorded while operating with a nanofluid is also found to be lower compared to that of water.

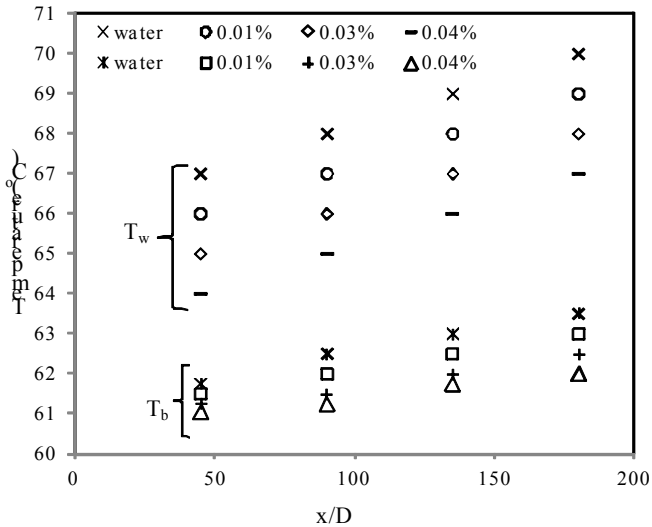


FIGURE 4. VARIATION OF WALL AND BULK FLUID TEMPERATURES AGAINST DIMENSION LESS LENGTH

Figures 5 and 6 show the variations of the convective heat transfer coefficient and Nusselt number against the Reynolds number. It is observed that the heat transfer coefficient increases with the increases in particle concentration and flow rate. The enhancement in convective heat transfer coefficient of the nanofluid over the base fluid is significant at higher Reynolds numbers. For example at a Reynolds number of 25000 and volume concentration of 0.04%, an enhancement of 18.14% ($Nu = 170$) has been observed compared to that of 8.41% ($Nu = 141$) when the Reynolds number is 5000 at the same volume concentration. The percentage enhancements in the heat transfer coefficient are 12.2%, 16.17%, and 18.4% at 0.01%, 0.03%, and 0.04% volume concentrations, respectively. The enhancement in the heat transfer is due to the quick

development of the hydraulic and thermal fields compared to that in laminar flow. The intensification of turbulence (eddy formation) also plays a vital role in high heat transfer rates, along with the addition of nanoparticles to the base fluid. The enhancement of the heat transfer coefficient directly depends on the thermal conductivity and indirectly on the thermal boundary layer thickness. Thermal conductivity of the nanofluid increases with increase in volume concentration. Decreasing of the thermal boundary layer thickness may be due to the mobility of particles near the wall, their migration to the center of tube, and reduction of viscosity at the wall region.

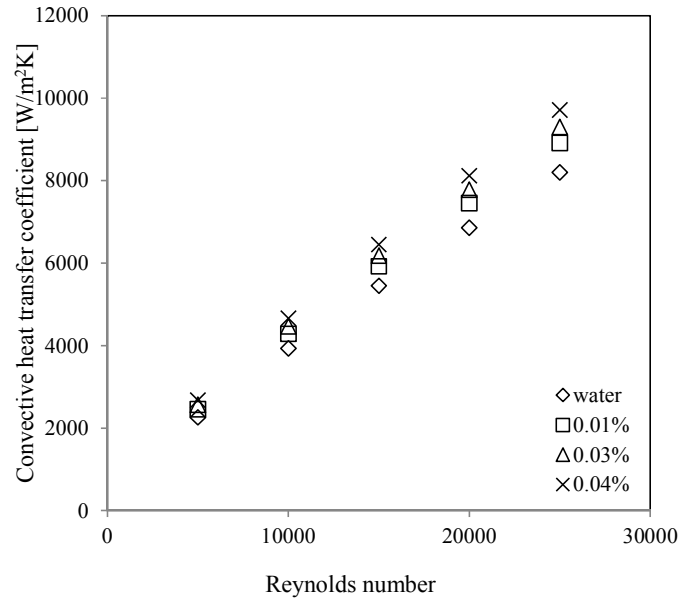


FIGURE 5. VARIATION OF AVERAGE HEAT TRANSFER COEFFICIENT WITH RESPECT TO REYNOLDS NUMBER

TABLE 2. $F_R(\tau\alpha)$ AND $F_R U_L$

Fluids	$F_R(\tau\alpha)$	$F_R U_L$ (W/m ² K)
Water	0.67	6.75
0.01% Silver/water nanofluid	0.7212	5.02
0.03% Silver/water nanofluid	0.7103	4.89
0.04% Silver/water nanofluid	0.7042	4.04

Figure 7 shows a typical Hottel-Whittier-Bliss performance characterization of the collector, which expresses the collector's efficiency as the fraction of incident radiation that is collected by the working fluid as per the ASHRAE 93-86 standards [20]. In the present study, it is observed that, at a flow rate of 6 L/min, the efficiency operated with nanofluid with a 0.04% volume concentration and the water efficiency is found

to be 68.7% and 60.7%, respectively. The main reason for this increase in efficiency can be explained by considering the two parameters, namely, the energy absorbed parameter $F_R(\tau\alpha)$ and the removed energy parameter, $F_R U_L$. Table 2 shows the $F_R(\tau\alpha)$ and $F_R U_L$ values of water and other concentrations of nanofluids. In the case of high circulation rates of the fluid, the smaller the temperature change from inlet to outlet and the closer the inlet fluid temperature to the average collector plate temperature, then the higher the value of the parameter F_R , for nanofluids. This value of F_R at a flow rate of 6 L/min is found 0.94, 0.91, and 0.89 for $\phi = 0.04\%$, 0.03% , and 0.01% , respectively, and compared to water, where the F_R value is 0.87. The energy absorbed parameter $F_R(\tau\alpha)$ is dominant in lower temperature rises corresponding to $((T_{fi} - T_a) / I_T) \times 1000 < 20$ and the removed energy parameter $F_R U_L$ is dominant in higher temperature differences. The $F_R(\tau\alpha)$ values for lower concentrations (0.01% and 0.03%) nanofluids would be greater than those of a higher concentration nanofluid (0.04%) at lower and higher temperature differences, as for $((T_{fi} - T_a) / I_T) \times 1000 < 20$, the $F_R U_L$ value for 0.04% nanofluid would be higher than 0.03% and 0.01% volume concentration nanofluids. Therefore, the efficiency of these ranges would be higher for 0.04% volume concentration nanofluid.

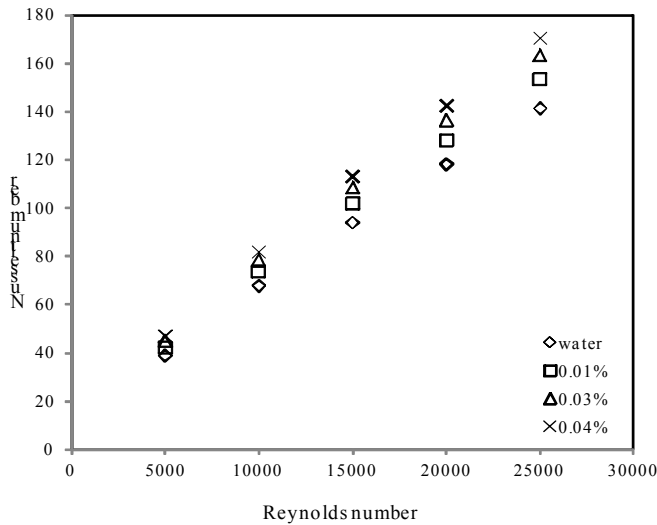


FIGURE 6. VARIATION OF AVERAGE NUSSELT NUMBER WITH RESPECT TO REYNOLDS NUMBER

This similar trend is observed by Yousefi et al. [15]. The thermal conductivity of nanofluid increases with increases in temperature and particle concentrations, and for higher temperatures, the thermal conductivity enhancement of the 0.04% nanofluid would be higher compared to two other concentrations, $\phi = 0.01\%$ and 0.03% . Moreover, the chaotic movement of the nano-particles suspended in the base fluid promotes thermal conductivity, and such chaotic movement is more dominant in the 0.04% volume concentration silver/water

nanofluid. By increasing the particle concentration, the effect in temperature rise becomes important.

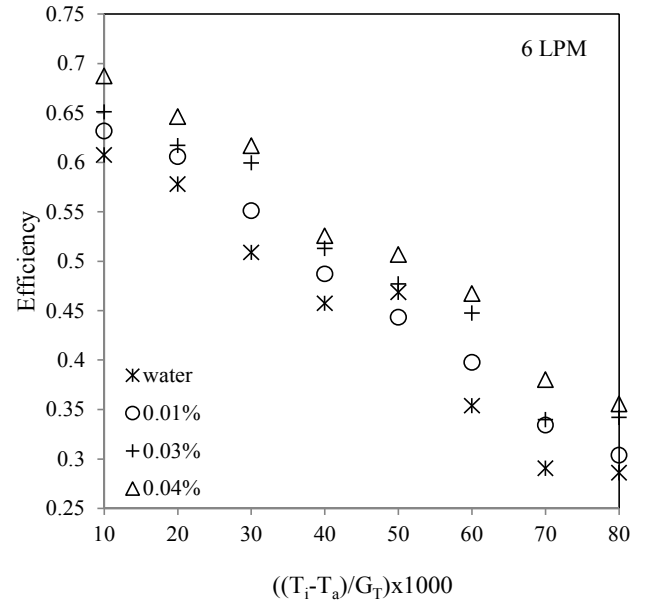


FIGURE 7. THE EFFICIENCY OF THE SOLAR FLAT PLATE COLLECTOR AT THE FLOW RATE OF 6 LPM

TABLE 3. EFFICIENCY PARAMETERS FOR WATER, $I_T = 800 \text{ W/m}^2$

$T_{fi} (\text{°C})$	40	50	60	70	80	90
$U_T (\text{W/m}^2\text{K})$	4.07	4.15	4.48	4.94	5.02	5.29
$Q_u (\text{W})$	945.2	800.34	736.83	675.2	634.72	441.21
$T_{fo} (\text{°C})$	51.24	59	68.4	78	87.5	94.25
$\eta_i (\%)$	58.24	50.15	46.49	42.27	39.65	27.64

Mass flow rate = 0.02 kg/s, $I_T = 800 \text{ W/m}^2$, water

Table 3 shows that the efficiency of the collector decreases sharply with the increasing values of the fluid inlet temperature T_{fi} , as the value falls from 60% to 29% as T_{fi} increases from 40°C to 90°C. This decrease is caused by the higher temperature level at which the collector as a whole operates when the fluid inlet temperature increases. Because of this the top-loss coefficient (U_T) and the surroundings' temperature increased difference, the heat lost increases and the heat gain decreases.

Comparing table 3 and table 4, it is seen that the useful heat gain is higher for nanofluids and so the efficiency of nanofluids over water is higher. This efficiency increases with increasing incidents of solar flux. The fluid inlet temperature and ambient temperature essentially determine the losses from a collector. Similarly, when the incident radiation flux increases, the useful heat gain and efficiency increase (table 5).

TABLE 4. EFFICIENCY PARAMETERS FOR 0.04% NANOFUID AT $I_T = 800 \text{ W/m}^2$

T_{fi} (°C)	40	50	60	70	80	90
U_T (W/m ² K)	3.87	3.95	4.08	4.14	4.22	4.49
Q_u (W)	1061.2	925.34	784.24	715.2	668.24	464
T_{fo} (°C)	53	62	69.3	78.54	87.64	96
η_i (%)	60.24	54.15	49.49	44.67	41.75	29.64

Mass flow rate = 0.02 kg/s, $I_T = 800 \text{ W/m}^2$, 0.04% silver/water nanofluid

TABLE 5. EFFICIENCY PARAMETERS FOR 0.04% SILVER/WATER NANOFUID AT $I_T = 1000 \text{ W/m}^2$

T_{fi} (°C)	40	50	60	70	80	90
U_T (W/m ² K)	3.87	3.95	4.08	4.14	4.22	4.49
Q_u (W)	1253.4	1090.18	1006.24	922.46	835.6	584.92
T_{fo} (°C)	55.4	63	72	81	90	97
η_i (%)	62.24	55.15	50.49	46.42	42.75	31.64

Mass flow rate = 0.02 kg/s, $I_T = 1000 \text{ W/m}^2$, 0.04% silver/water nanofluid

Figure 8 shows the variations of pressure drops against the Reynolds number for the different particle concentrations. Pressure drop is found to increase as the particle volume concentration increases, which is primarily due to the increase in viscosity. The increase is more dominant for higher Reynolds numbers; for example, at Reynolds number of 25000 and 0.04% volume concentration, the pressure drop is 67.24 kPa, whereas in the case of water the pressure drop is 62.48kPa, which is a 7.5% increase in pressure drop. For a Reynolds number between 10000 and 15000, the pressure drop increases are 6.45%, 5.25%, and 3.17% for 0.04%, 0.03%, and 0.01% volume concentrations, respectively. It is observed from the present study that the Reynolds number is to be maintained between 10000 and 15000 for low pumping power and best efficiencies.

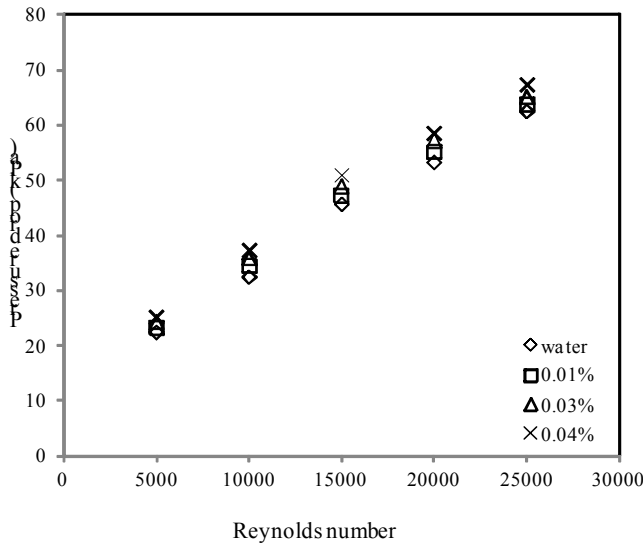


FIGURE 8. VARIATION IN PRESSURE DROP WITH RESPECT TO REYNOLDS NUMBER.

4. CONCLUSION

The performance characteristics of a solar flat-plate collector operated with silver/water nanofluid is experimentally investigated and the effect of the nanofluid on the efficiency of the collector is compared with that of water. The particle volume concentration increases the convective heat transfer rate, and the maximum percentage increase obtained is 18.4% under the tested condition. Similarly, the efficiency of the flat-plate collector is found to increase with increasing particle concentration and flow rate. The maximum efficiency of the system is found to be near 70% for 0.04% particle volume concentration at 6 L/min. The primary reason for the enhancement in the heat transfer coefficient is due to the enhanced thermal conductivity of the suspended nanoparticles.

NOMENCLATURE

- A Area, m²
- C_p Specific heat capacity, J/Kg K
- D Diameter, m
- F_R Heat removal factor
- h Convective heat transfer coefficient, W/m²K
- I_T Total/Global radiation, W/m²
- k Thermal conductivity, W/mK
- l Length, m
- Nu Nusselt number
- q Heat flux, W/m²
- Q Heat flow, W
- Re Reynolds Number
- S Absorbed radiation, W/m²
- T Temperature, °C
- U_T Natural convective heat transfer coefficient, W/m²k
- u velocity, m/s

Subscript

- a ambient temperature
- b bulk fluid temperature
- c collector

bf	base fluid
f_i	fluid inlet temperature
nf	nanofluid
p	collector plate area
p	nanoparticle
pm	mean plate temperature
t	riser tube
w	wall
u	useful
i	initial
fo	fluid outer
l	loss

Greek symbols

β	nano layer thickness to original particle radius
\emptyset	volume fraction
ρ	density, kg/m ³
μ	dynamic viscosity, kg/m s

ACKNOWLEDGMENTS

The fifth author would like to thank the National Science and Technology Development Agency, and the National Research University Project for the supporting. The authors would like to thank Mr. Seelan, Mr. P. Augustine and Mr. Jeyakumar of Karunya University for helping in the fabrication of the experimental test facility.

REFERENCES

1. L.G.Asirvatham, Enhancement of heat transfer using nanofluids - An overview, Renewable and Sustainable Energy reviews,Chennai-629-641 (2009) Vol. 14.
2. S.U.S Choi, Z.G.Zhang, W.Yu, Anomalous thermal conductivity enhancement in nanotube suspensions.: Applied Physics Lett, Vol. 79 (14) (2001) 2252.
3. S.U.S Choi,Nanofluids: from vision to reality through research, Journal of Heat transfer, Vol. 131 (2009)3: 1-9.
4. S.U.S.Choi, Z.G.Zhang and P.Keblinski, Nanofluids, Encyclopedia of Nanoscience and Nanotechnology, Vol. 6.737-757.
5. W.Yu, D. M France, J.L Routbort, and S.U. S. Choi, Review and comparison of nanofluid thermal conductivity and heat transfer enhancements,Heat transfer Engineering, (2008) Vol. 29.5 432-460.
6. T.Tyler,O.Shenderova,G.Cunningham,J.Walsh,J.Drobnik and G.McGuire,Thermal transport properties of diamond based nanofluids and nanocomposites Diamond and related materials, Vol. 15 (2006)11-12, 2078-2081.
7. S.K.Das, S.U.S. Choi, and H.E. Patel Heat transfer in nanofluids - a reviewHeat transfer Engineering, Vol. 27 (2006) 10:3-19.
8. M.S.Liu, M.C.C Lin, L.T.Huang and C.C Wang, Enhancement of thermal conductivity with carbon

- nanotube for nanofluids, International Communications in Heat and Mass transfer (2005) Vol. 32.1202-1210
9. V.Kaufui, Wong, and Omar De Leon, Applications of Nanofluids: Current and Future, Article ID 519659,Advances in Mechanical Engineering, Vol. 2010.
10. G.Donzelli, R.Cerbino and A.Vailati, Bistable heat transfer in a nanofluid, Article ID 104503, Physical Review Letters, 2009, Vol. 102.
11. S.J.Kim, I.C.Bang, J.Buongiornio and I. W. Hu, Study of pool boiling and critical heat flux enhancement in nanofluids,Bulletin of the polish Academy of Sciences - Technical Sciences, Vol. 55.2 211-216,
12. H.B.Ma, C Wilson, Q. Yu, K. Park, S.U.S.Choi, An experimental investigation of heat transport capability in a nanofluid oscillating heat pipe,Journal of Heat transfer, Vol. 128.11 1213-1216,
13. Mahian et al, A review of applications of nanofluids in solar energy. International Journal of Heat and Mass Transfer 57 (2013) 582–594.
14. Hua Qing Xie, Wei Yu, Jing Li, Yang Li, Investigation on Heat Transfer Performances of Nanofluids in Solar Collector,Materials Science Forum (Volume 694), Vol. Frontier of Nanoscience and Technology (2011) 33
15. Tooraj Yousefi, Farzad Veysia, Ehsan Shojaeizadeha, Sirus Zinadinib. Kermanshah, An experimental investigation on the effect of Al₂O₃-H₂O nanofluid on the efficiency of solar flat plate collectors, Iran Renewable Energy Journal (2011) Vol. 39 293- 298.
16. H.Tyagi, P.Phelan, R.J.Prasher, Predicted efficiency of a low-temperature nanofluid based direct absorption solar collector, Sol Energy Eng (2009) 131:0410041e7
17. Taylor A. Robert, Patrick E.Phelan, Todd P.Otanicar, Chad A.Walker, Monica Nguyen, Steven Trimble, Ravi Prasher,Applicability of nanofluids in high flux solar collectors. 023104-1, Tempe, Arizona : Journal of Renewable and Sustainable energy (2011) Vol. 3.
18. Dongxiao Han, Zhaoguo Meng, Daxiong Wu, Canying Zhang and Haitao Zhu, Thermal properties of carbon black aqueous, Nanoscale Research Letters (2011) 6:457
19. Lijuan Mu, Qunzhi Zhu, Leilei Si, Radiative Properties of Nanofluids and Performance of a Direct Solar Absorber Using Nanofluids, Paper no. MNHMT2009-18402 pp. 549-553 , Vols. ASME 2009 Second International Conference on Micro/Nanoscale Heat and Mass Transfer, Volume 1 (2009).
20. ASHRAE Standard 86-93. Methods of testing to determine the thermal performance of solar collectors; 1986. Atlanta, GA, USA.
21. B.C Pak, Y.I Cho,Hydrodynamic and heat transfer study of dispersed fluids with sub micron metallic oxide particles,Exp. Heat Transfer 11(1998) 151.

22. W.Yu ,S.U.S Choi,The role of interfacial layers in the enhanced thermal conductivity of nanofluids; a renovated Maxwell model .J.Nanoparticles res 5 (2003) p.167.
23. D.A Drew, S.L PassmanTheory of multicomponent fluids, Springer Berlin (1999).
24. Y.Xuan. W.Roetzel, Conceptions for heat transfer correlation of nanofluids, Int.J. Heat Mass Transfer 43 (2000) 3701.
25. Robert J. Moffat, Describing the Uncertainties in Experimental Results, Experimental Thermal and Fluid Science 1988; 1:3-17.
26. P.W.Dittus, and L. M. K. Boelter, Heat transfer in automobile radiators of the tubular type Univ. Calif.Pub. Eng., Vol. 2, No. 13, pp. 443-461 (1930), reprinted in Int. Comm. Heat Mass Transfer, Vol. 12 (1985) pp. 3-22.
27. H.C.Hottel, W.Whillier, Evaluation of flat plate solar collector performance. Trans. Conf. Use of Solar Energy Thermal Processes. Tuscon AZ.(1955).
28. R.W.Bliss, The derivation of several “plate efficiency factors” useful in the design of the flat plate solar heat collector. Solar Energy. Vol 4 (1959) pp55-64.